J. Jpn. Soc. Powder Powder Metallurgy, **72** (2025) S745-S752
https://doi.org/10.2497/jjspm.15E-SIS13-06

Direct Recycling of Tool Steel Swarf using Field Assisted Sintering

Monica KESZLER[1]*, Felix GROSSWENDT[2], Anna-Caroline ASSMANN[3], Arne RÖTTGER[4], Sebastian WEBER[2], Olivier GUILLON[1], and Martin BRAM[1,2]

[1]Forschungszentrum Jülich GmbH, Wilhelm-Johnen-Strasse, Jülich 52428, Germany
[2]Ruhr-Universität Bochum, Lehrstuhl Werkstofftechnik, Universitätsstraße 150, 44801 Bochum, Germany
[3]RWTH Aachen, Lehrstuhl für Anthropogene Stoffkreisläufe, Intzestrasse 1, 52072 Aachen, Germany
[4]Bergische Universität Wuppertal, Lehrstuhl für neue Fertigungstechnologien und Werkstoffe, Bahnhofstr. 15, 42651 Solingen

Abstract
Steel swarf generated from the machining and polishing of steel tools can be recovered, cleaned, milled, and magnetically separated into a powder suitable for processing via field assisted sintering. Field assisted sintering, when combined with thermal post-treatments, has the potential to directly generate tools, such as cutting disks, from this recovered swarf. The attractive features of this technique include the ability to generate metal matrix composites, the utilization of unconventionally shaped powder, and the avoidance of the high energy cost of re-melting. The possibilities of this technique are explored using a high carbon and high chromium steel swarf, AISI D2, produced industrially and recovered for direct recycling to contribute to a circular economy.

Keywords: Recycling, tool steel, field assisted sintering, circular economy

Introduction

In shaping steel tools to their final form, grinding is an often-utilized technique, creating swarf of a small particle size. In the case of other forms of machining, such turning or milling, steel swarf is produced that has a larger particle size (mm scale). With this large particle size, these metallic chips can be pressed in order to remove residual cutting fluid and be reused in steel production [1)]. Recycling of larger steel chips is already performed at the industrial scale through re-melting and using it for new steel production [2)]. Grinding chips, however, are often much smaller than chips from turning or milling (µm scale). Even if these chips were pressed to remove grinding lubricant, the morphology of the grinding swarf can often lead to the formation of aggregates that trap abrasive grinding particles and residual cooling lubricant [3–5)]. The trapped lubricant can be cost intensive to remove, as the most viable techniques available are based on lubricant combustion or cleaning via supercritical CO_2 [6–8)]. In combination with melting metallurgical processes, used to further recycle the swarf, the overall recycling process of swarf from grinding sludge becomes energy intensive as well. Therefore, grinding sludge is presently sent directly to landfill. This choice has its own downsides, as grinding lubricant and metallic swarf can be harmful to human and environmental health along with incurring significant costs for landfilling [2,6)].

The worldwide push for greener technology and furthering a more circular economy has led to renewed interest in recovering steel from grinding sludge as opposed to disposing of it entirely [9)]. Environmental regulations and geopolitical supply risk have also elevated the subject of steel recovery and recycling to the forefront [10,11)]. In this work, focus is placed on a single stream of tool steel, specifically X153CrMoV12 (AISI D2), referred to from here as D2. D2 contains high contents of Cr and V, elements of high demand for steel production [12)]. This tool steel has high wear resistance and non-deforming properties, therefore making it attractive for cutting applications [13)].

In this work, the goal of recovering D2 steel from its sludge to use as a starting material for field assisted sintering technique/spark plasma sintering (FAST/SPS) to directly form a cylindrical part, which could be used as a cutting disk. FAST/SPS is a powder metallurgical technique that involves sintering the metal particles together into a consolidated piece. It avoids the high energy cost of melting metal, as the consolidation occurs below the melting temperature [14,15)]. FAST/SPS functions through the application of uniaxial pressure and a pulsed current to powder that has been placed within a conductive die. Through the application of the current, the die and the powder both heat up via Joule heating, leading to a high heating rate. This high heating rate allows for fast mass transfer and rapid consolidation [16)]. The unique method of FAST/SPS leads to sintering times much lower than needed to sinter powder in comparison to conventional sintering, i.e., sintering occurs in minutes as opposed to hours [17,18)].

Another benefit of sintering with FAST/SPS is the possibility for mixed materials to be sintered together, leading to a composite with a secondary phase such as additive hard particles suspended in the matrix [19)]. The D2 sludge utilized within this work had minimal cleaning steps prior to its sintering, but removal of its water-based lubricant was performed via drying and some magnetic separation was performed. High amounts of Al_2O_3 and SiC abrasive particles are left within the swarf, even after the industrial scale magnetic

*Corresponding author, E-mail : m.keszler@fz-juelich.de

separation via magnet rolls. Therefore, the swarf is rather impure, and the corundum particles will become trapped within the matrix of steel during sintering.

In general, FAST/SPS offers other advantages including potentially breaking down oxide layers on metallic particles [17,20], using significantly less energy than hot-pressing [21], and consolidating irregularly shaped powders into fully dense parts [22]. As D2 swarf is an unconventional powder metallurgical material due to its spiral-like shape and high contamination with abrasive particles, FAST/SPS is an attractive candidate in handling the D2 swarf without the need for elaborate pre-processing. Besides this, it is possible that an extended FAST/SPS cycle could lead to an ideal austenitization of contaminated D2 steel. In combination with high cooling rates after sintering, subsequent quenching steps could potentially be avoided. Austenitization is important for maternsite formation as the basis of controlled carbide precipitations by subsequent thermal treatments.

As the FAST/SPS process primarily uses cylindrical dies, D2 is sintered via FAST/SPS with the aim of generating upcycled cutting disks. Investigating the production of disks from the considered D2 recyclate by FAST/SPS processing, paves the way for the sintering of other potential tool steel powders in the production of other parts with a low shape complexity. This work discusses the integration of hardening within FAST/SPS processing by varying the process duration at a sintering temperature above the austenitizing temperature of D2 recyclate for potential use in a cutting disk.

Experiment

D2 powder analysis

D2 powder used in this study was delivered by Bergische Universität Wuppertal from previous studies on the FAST/SPS sintering of D2 swarf [23]. The considered recyclate powder originates from the production of circular knives made of AISI D2 cold work tool steel. The grinding process is performed using grinding wheels containing both Al_2O_3 and SiC along with a water-based cooling lubricant. The grinding swarf supplied was dried and magnetically separated. Particle morphology was analyzed via field emission gun scanning electron microscopy (referred to in this work as SEM) using a Zeiss Gemini 450 (Carl Zeiss AG, Germany) operated with an acceleration voltage of 8 kV and working distance of 8.0 mm. A classical Everhardt-Thornley detector was used to image the powder morphology. Phase diagrams were calculated via ThermoCalc TCFE10 (Thermo-Calc Software AB, Sweden) with phases FCC A1 (austenite), BCC A2 (ferrite), FCC A1#2 (MC), M_7C_3, $M_{23}C_6$, Graphite (in the case of recyclate sintered via FAST/SPS) and liquid.

FAST/SPS sintering for austenitized D2

5 g of the D2 grinding waste was poured into a 20 mm diameter graphite mold (SGL Carbon, SIGRAFINE R7710). The graphite mold was lined with 0.38 mm thickness carbon foil that was sprayed with boron nitride spray at all contact points with the steel to mitigate carbon diffusion. FAST/SPS was performed in an HP-D5 device (FCT Systeme GmbH, Rauenstein, Germany) with a heating rate of 100 K/min, maximum temperature of 950 °C, and an uniaxially applied pressure of 50 MPa. Samples varied in their dwell time at maximum temperatures, with samples sintered with 1-, 5-, 10-, and 20-minute dwell times at 950 °C. After a 10-minute cooling period to room temperature, samples were extracted with a hand press and cleaned of their graphite foil with a knife prior to sandblasting.

Heat treatment and metallographic procedure

The density of the cleaned samples was determined by the Archimedes method using ethanol as the fluid medium. The sintered samples were then cut in half using a cBN cut-off wheel. One half of each sample was subjected to heat treatment consisting of triple tempering in the regime of secondary hardness at 540 °C in a convection furnace. The other half was not heat treated and left in as-sintered condition. The samples were then embedded in electrically conductive resin to be ground and polished. Subsequently, retained austenite (RA) contents were determined at the cross-sections by X-ray diffraction using a type μ360-x (Pulsetec, Japan). Afterwards Vickers hardness testing (HV30) was performed using an automated hardness tester type KB30s (KB Prüftechnik, Germany). To investigate the microstructures, the cross-sections were etched using Nital (3%) prior to SEM investigation. To investigate the uptake of C during FAST/SPS of the samples, carrier hot gas extraction (HGE) was performed. 300 to 500 mg of sample mass taken from the sample bulk were analyzed within one measurement. The global C contents given are the averages of three individual measurements C contents were measured using a type CS-800 by Eltra (Germany) while measurement of N and O contents were performed using a type TCH 600 by Leco (USA). For microstructural analysis, secondary electron (SE) and back-scattered electron (BSE) analysis was performed with a MIRA3 Tescan SEM (Tescan Group, Czech Republic) using an acceleration voltage of 15 kV and a working distance of 15 mm. D2 reference samples of both cast and powder metallurgical origin (Dörrenberg Edelstahl GmbH, Germany) were also prepared and analyzed via SEM using a Coxem EM-30N (Kosdaq Company, Korea) at an acceleration voltage of 10 kV and working distance of 15 mm.

Results and Discussion

D2 recyclate powder properties

As seen in Fig. 1, the D2 grinding chips display a tendril-like morphology that can easily trap air when compressed into a mold.

These spiral shapes also trap grinding medium, such as Al_2O_3. The shape of this powder led to issues with compacting the material into FAST/SPS dies. Therefore, only a small amount of 5 g could effectively be compressed into the 20 mm die for FAST/SPS sintering. The chemical composition of the powder is given in Table 1. According to the ASTM A681 standard, the C content of D2 is limited to 1.4 to 1.6mass% [24]. The chemical composition of the grinding swarf of D2 used as a starting powder in this work differs for a number of reasons. Increased C content can be attributed to residual organics from the water-based grinding lubricant, along with the presence of SiC from the grinding wheels. The N content in the waste likely comes from reaction with the air, presence of other grinding medium, or organics that shed from the grinding wheels themselves.

The hypothesis regarding sufficient austenitization for an integrated hardening of the D2 grinding waste during FAST/SPS originated from the phase diagram shown in Fig. 2. Fig. 2a shows the phase diagram for virgin D2 steel, while Fig. 2b. is a recalculated phase diagram for the D2 grinding waste, which considers the variation in C content , along with Si and N contamination from the grinding process. The grey region marks the Austenite+M_7C_3 domain, which is desired for hardening. The deviation of this grey region between Fig. 2a and Fig. 2b can be attributed to the altered chemical composition. Due to the increased C-content of the recyclate material, austenitizing can be realized at the considered sintering temperature of 950 °C. This temperature is relatively low compared to typical D2 hardening temperatures between 1030-1080 °C.

Full austenitization is not possible for D2 steel due to the presence of stable M_7C_3 carbides. Though full austenitization is not possible, ideal treatment of D2 would be done in such a way to prevent the retention of ferrite. If ferrite is retained during the austenitizing, it cannot be transformed into martensite during quenching. As the D2 grinding swarf contains a C content of over 3wt%, it is not possible to achieve an ideal phase composition at any treatment temperature. During the FAST/SPS process, residual organics are burnt off resulting in a lowered C content. If this leads to a C content closer to 2.5wt% globally in the sintered state, the ideal treatment temperature range to enter the desired austenite+M_7C_3 domain would be around 950 – 1220 °C. As FAST/SPS is a sintering process that uses Joule heating as the primary heat source, with a setpoint of 950 °C, contact points between powder particles were expected to reach and maintain temperatures within this range [25]. Raising the maximum sintering temperature to 1000 °C or above caused a melt phase to form in previous investigations. This resulted in damaging the punches. Therefore, increasing the sintering temperature is not an option. Temperatures below 950 °C are expected to lead to the retention of ferrite and therefore need to be avoided too in order to realize the desired austenitization state during FAST/SPS.

Table 1. – Chemical composition of D2 given by ASTM A681 and the measured composition of the starting powder in mass%. All elements determined by X-ray fluorescence spectrometry using a Niton XL2 air by Thermo Scientific (USA). *C content measured by HGE (CS-800 by Eltra (Germany)), **N and O measured by HGE (TCH 600 by Leco (USA)).

	C*	Si	Mn	Cr	Mo	V	Al	N**	O**	Fe
Nominal comp.	1.4-1.6	0.1-0.6	0.1-0.6	11.0-13.0	0.7-1.2	0.5-1.1	-	-	-	Bal.
Recyclate powder	3.19±0.03	3.92±0.59	0.41±0.01	10.90±0.05	0.68±0.01	0.72±0.03	2.90±0.06	0.11±0.01	0.884±0.07	Bal.

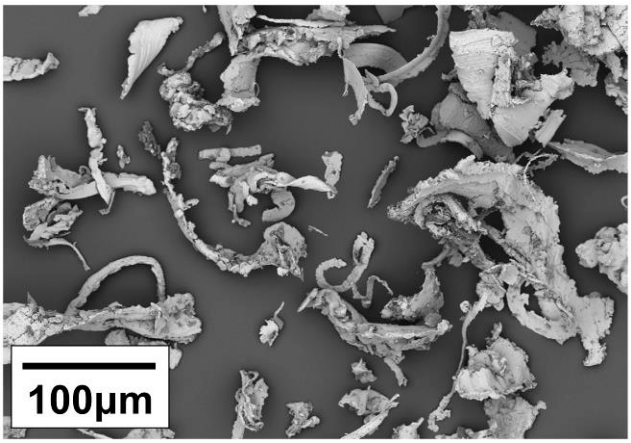

Fig. 1. – SEM image showing the powder morphology of the D2 grinding waste

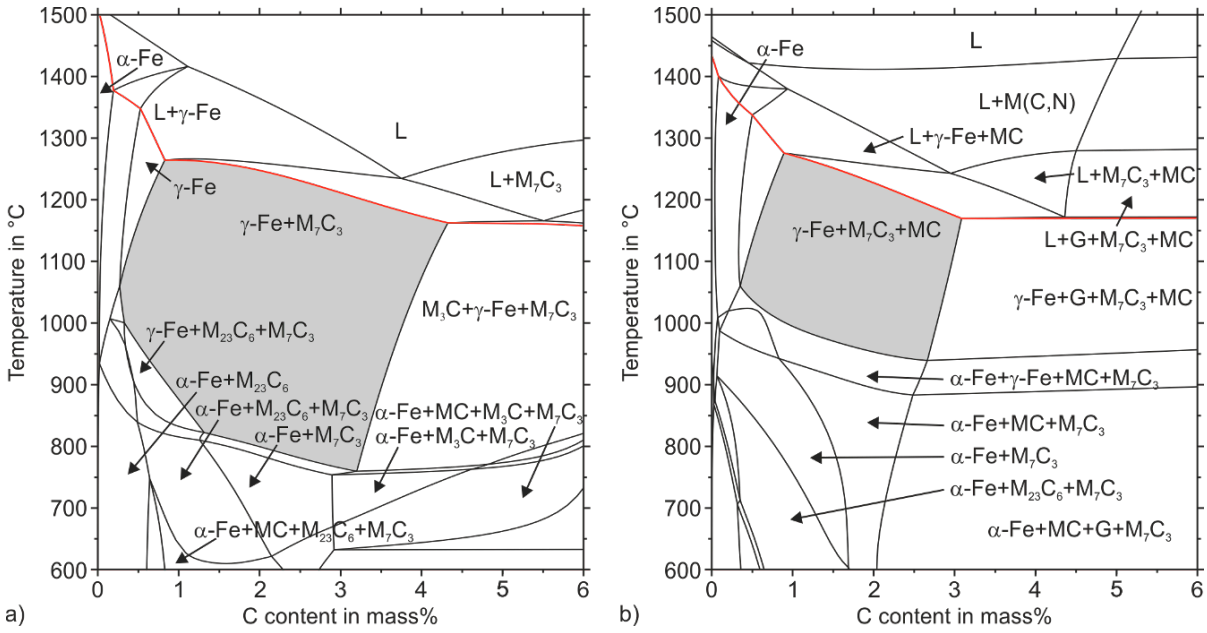

Fig. 2. – Phase diagrams of a) D2 steel and b) D2 steel grinding waste with C and N contamination considered. The grey region represents the ideal phase composition for hardening.

FAST/SPS austenitization and subsequent tempering

Table 2 displays the Archimedes density of the pellets after FAST/SPS sintering. At this scale, it appears that dwell time only has a slight effect on increasing the density of the pellets. When considering the density of D2 tool steel (7.7 g/cm^3) for density calculations, the highest relative density achieved is roughly 94% by the sample that dwells for 20 minutes. This differs by less than 1% from the sample that dwells for only 1 minute. Limited accuracy of D2 density calculation at this stage can be attributed to a number of reasons. Firstly, the primary reason for lower density than that of standard D2 is the presence of Al_2O_3 contamination. Al_2O_3 has a density of 3.99 g/cm^3, half of that of the D2 steel. The D2 grinding waste could contain roughly 10-15 mass% Al_2O_3 leading to a considerably lower density than pure D2, even with little to no porosity in the sintered samples. Secondly, the tendril-like particles may have resisted full compression during FAST/SPS leading to voids inside the sintered material. As the volume percentage of contamination will vary between samples, considering the starting powder is a waste product that has not been fully homogenized, variation in the densities is to be expected.

Table 2. – Density values for 20 mm D2 FAST/SPS sintered at 950 °C and various dwell times

FAST/SPS Sample	Density (g/cm^3)
20 mm, 1 min dwell	7.20±0.1
20 mm, 5 min dwell	7.19±0.1
20 mm, 10 min dwell	7.23±0.1
20 mm, 20 min dwell	7.24±0.1

Fig. 3 displays hardness and retained austenite content between as-FAST/SPS sintered samples and the same samples after heat treatment of tempering at 540 ◦C. Carbon content of as-FAST/SPS sintered samples is also included. In Fig. 3A, it is shown that the hardness of the as-FAST/SPS samples drops with the increased dwell time. This is likely due to increased solute C content in the matrix during the sintering process. Increase of solute C content could be attributed to the time dependent dissolution of SiC particles in the samples. With increased sintering time, more C can be released from the SiC particles, leading to higher solute C contents in the 10- and 20-minute dwell samples. This increase of solute C promotes higher RA amounts, which can be seen in Fig. 3B. It can be concluded that the excessive RA contents lead to the reduced hardness of the samples sintered with longer dwell times. As seen in Fig. 3C, the global C content of the samples is only slightly increased with increased sintering times from 2.46 to 2.52 mass% C. This shows that, despite the fact that all sintering was performed in graphite tools, the protective BN coating on the graphite foil is effectively preventing excess C from dissolving into the steel during the sintering process. Direct tempering transforms the majority of RA, as can be seen by the steep difference in austenite percentage between the as-FAST samples and the tempered samples in Fig. 3B. Because samples with longer sintering times produced more RA, the tempering of the samples with longer dwell times led to better hardness post-tempering, due to the promotion of tempering carbide formation. The 20-minute dwell sample reached the

highest hardness of the considered samples of roughly 680 HV30 after direct tempering.

Prior to tempering, all as-FAST/SPS samples showed higher hardness. This may be due to a congregation of carbides at the surface of the samples, higher solution state of alloying elements, or higher dislocation density due to the rapid heating and cooling during the FAST/SPS process. Tempering may have promoted dispersion of carbides and reduction of dislocations and residual stresses, thus leading to a lower sample hardness. But this trade-off likely increased the toughness of the material at the expense of its hardness. Unfortunately, all of these samples fail to reach the Vickers hardness value of cast reference material (713 HV30). This could be due to unwanted retention of ferrite prior to tempering as well as residual porosity after FAST/SPS.

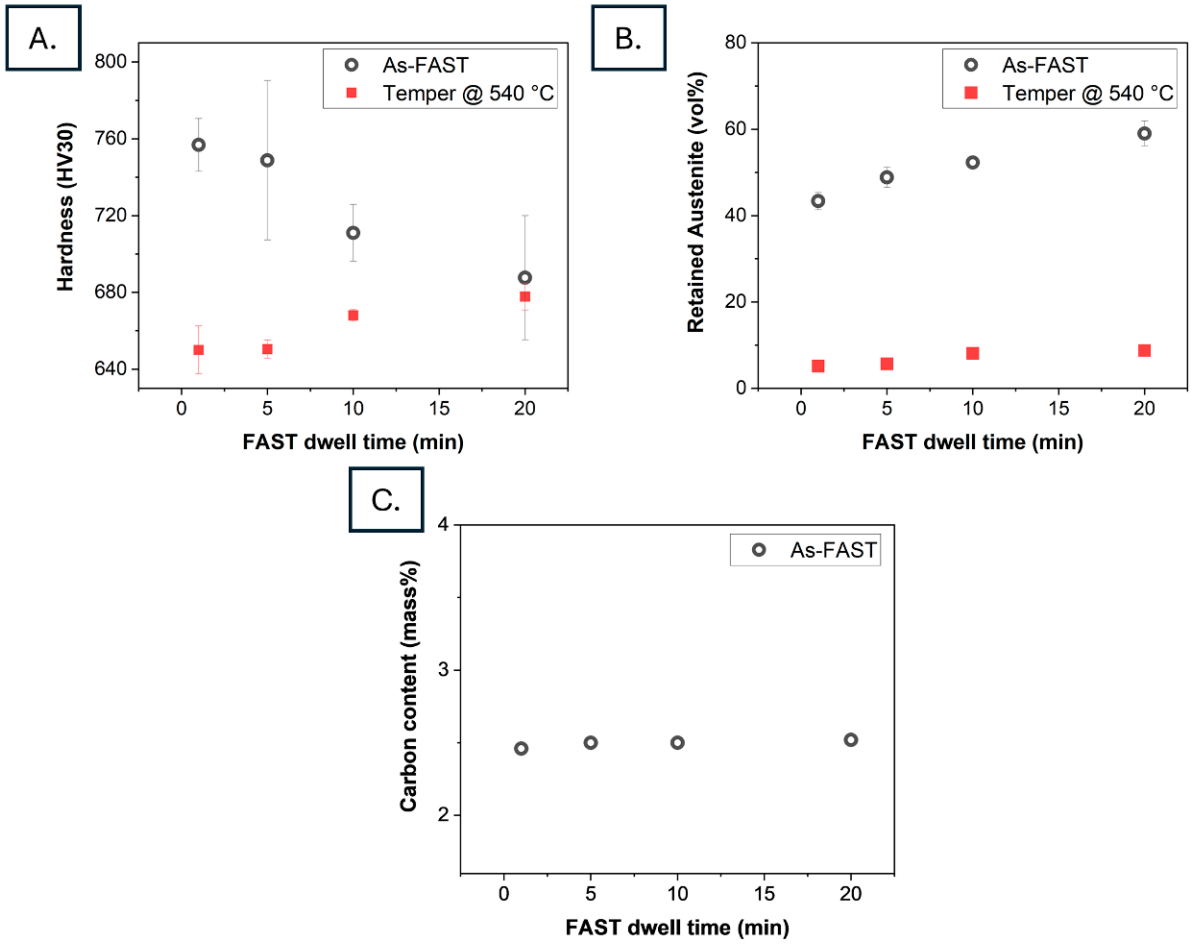

Fig. 3. – Graphs showing the difference between 20 mm as-FAST/SPS samples and samples tempered at 540 C in A.) hardness (HV30), B.) retained austenite content (vol%), C.) carbon content (mass%, as-FAST/SPS only)

Fig. 4 and 5 show SEM images of the samples sintered with a 1-minute and 20-minute dwell, respectively, before and after tempering. Both samples show Al_2O_3 captured within the matrix of steel, most easily seen through the SE images as regions of high charge due to their lack of conductivity. Both samples also display contamination of SiC, seen as the brightly ringed regions in the SE images. In Fig. 4A and B, dissolution of SiC does not seem to be occurring as readily as between Fig. 5A and B, as the 20-minute dwell sample shows more pronounced dissolution than the 1-minute sample. This can be seen through the softer edge of the SiC contamination, especially in the upper left corner of Fig. 5A. After the triple tempering at 540°C for 2h, dissolution has continued, but still not to completion. Fig. 5B still shows a segregated SiC region in the upper left corner of the images. The localized contribution of C from the dissolution of SiC particles is part of the reason for the variation in hardness and RA content between the samples .

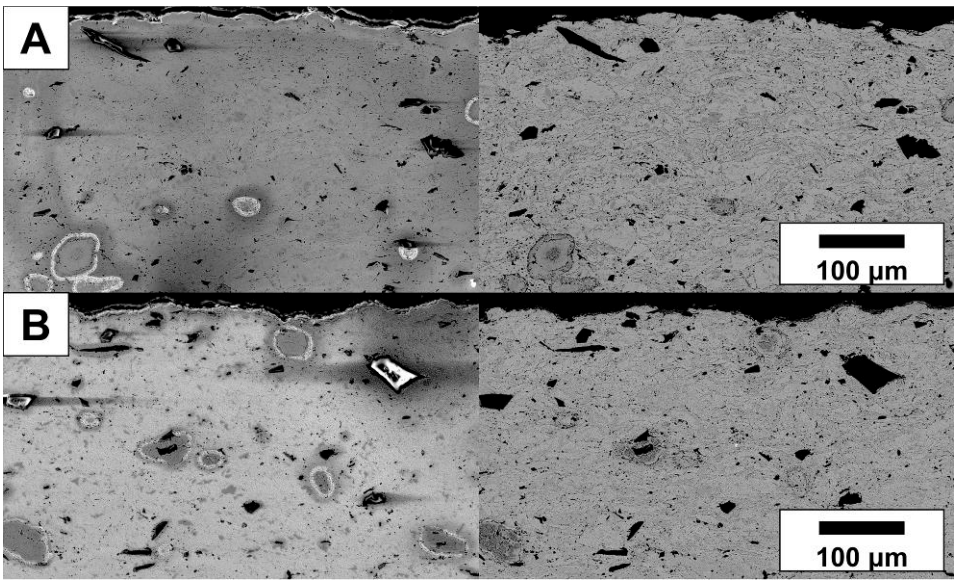

Fig. 4 – SE (left) and BSE (right) SEM images of D2 waste A. directly after FAST/SPS sintering with 1-minute dwell and B. after tempering

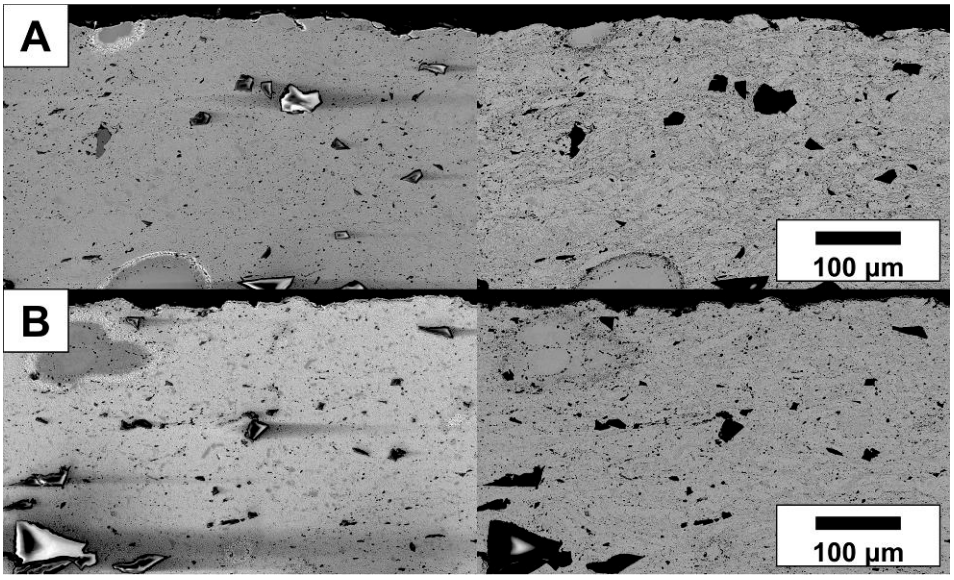

Fig. 5 – SE (left) and BSE (right) SEM images of D2 waste A. directly after FAST/SPS sintering with 20-minute dwell and B. after tempering

Fig. 6 shows a comparison between BSE SEM images of industrial cast and hot formed D2, the D2 recyclate after 20-minute FAST/SPS sintering and tempering, and an industrial powder metallurgical D2 sample. The D2 waste processed in this work is generated from cast material like displayed in Fig. 6A. The dark regions seen in Fig. 6B represent both Al_2O_3 contamination and the presence of oxides. In contrast, as Fig. 6C comes from a sample generated from D2 powder made specifically for powder metallurgy, the SEM analysis shows only few oxides in this sample. The dark grey regions seen in all three images are Cr-rich carbides. For the powder metallurgical D2 these carbides are <10 µm, round, and fairly evenly distributed through the steel matrix (Fig. 6C). The carbides of the melting metallurgical sample and the FAST/SPS-processed recyclate exhibit a larger size. The carbides in the cast and hot formed D2 sample are arranged in lines parallel to the rolling direction. The carbides are of blocky, sharp-edged shape due to the fragmentation during hot forming. Individual carbides exhibit lengths of 50 to 100 µm (Fig. 6A). Contrary, the FAST/SPS processed grinding swarf shows a more even dispersion of the carbides. Owing to the grinding process and the subsequent sintering, these carbides appear smaller and more rounded. Therefore, the carbide distribution and morphology of the FAST/SPS-processed swarf resembles that of the powder metallurgical D2 more than that of the melting metallurgical D2 from which the swarf originates, which is more optimal for mechanical performance. However, the presence of the sharp-edged Al_2O_3 particles that act inert and are not bonded with the steel matrix are expected to affect the toughness of the material in a negative way [26].

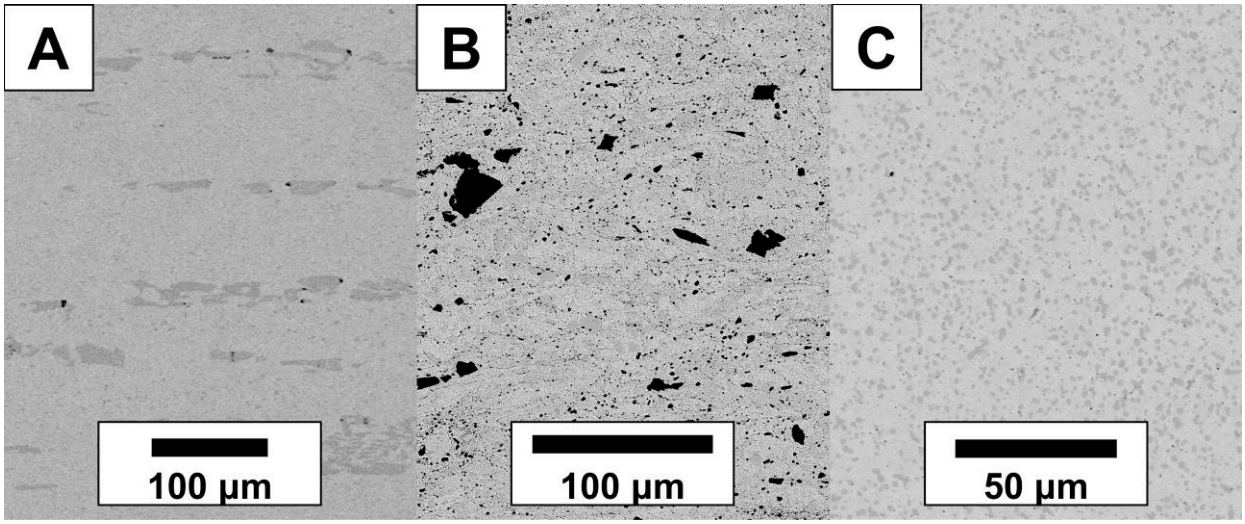

Fig. 6 – BSE SEM images of A. Cast and hot deformed D2 steel, B. D2 grinding waste FAST/SPS sintering with 20-minute dwell, and C. a powder metallurgically D2 produced sample. All samples are heat-treated in the regime of secondary hardness.

Conclusion

Increased dwell time during FAST/SPS sintering of D2 grinding waste leads to increased RA content within the sample. Initially, this lead to the samples with long dwell times having a lower hardness in as-FAST/SPS condition. However, direct tempering of the FAST/SPS samples transformed the high RA content. The high-RA samples developed a higher hardness than the samples with a lower starting austenite content. Thus, it could be shown that direct tempering of FAST/SPS sintered tool steel grinding waste can be performed without the need for additional austenitzing and quenching. However, the recycled D2 samples are not capable of achieving target hardness of 713 HV30 after direct tempering. The highest secondary hardness achieved was seen in the 20-minute dwell sample at 680 HV30 whereas the highest initial hardness after FAST/SPS was 760 HV30 after 1 minute dwell time. It can be assumed that the considered sintering temperature was slightly too low to avoid the retention of ferrite during austenitization by FAST/SPS-processing. Full dissolution of SiC contamination was also not realized, even with 20-minute dwell and subsequent tempering. Further improvement of the D2 FAST/SPS recyclate hardness would likely have to come from complete magnetic separation of the metal from the non-metal contaminants along with cleaning the powder from lubricant residue.

Acknowledgements

This research was done in the framework of the project “EnerGieeffziENtE KreiSlaufwirtschaft krItischer RohStoffe (GENESIS)“, which is funded by the German Federal Ministry for Economic Affairs and Climate Action (BMWK) according to a decision of the German Federal Parliament. The funding is highly acknowledged. GENESIS is a joint project between the Ruhr-Universität Bochum, the Bergische Universität Wuppertal, the RWTH Aachen and the Forschungszentrum Jülich as scientific institutions, the German companies WILO SE, Klaus Kuhn Edelstahl, August Berghaus GmbH, Berger Gruppe as end users and Glamatronic, OWL and Dr. Fritsch Sondermaschinen GmbH as equipment manufacturers. Experimental support of Ralf Steinert (FAST/SPS) and Denise Ramler (SEM) is highly acknowledged.

References

1) Li P., Li X., Li F., *J. Clean. Prod.*, **266**, 121732 (2020).
2) Lee C.-M., Choi Y.-H., Ha J.-H., Woo W.-S., *Int. J. Precis. Eng. Manuf.-Green Technol.*, **4**, 457–468 (2017).
3) Ramanath S., Ramaraj T. C., Shaw M. C., *CIRP Ann.*, **36**, 245–247 (1987).
4) Kopac J., Krajnik P., *J. Mater. Process. Technol.*, **175**, 278–284 (2006).
5) Ni J., Yang Y., Wu C., *J. Clean. Prod.*, **212**, 593–601 (2019).
6) Fu H., Matthews M. A., S. Warner L., *Waste Manag.*, **18**, 321–329 (1998).
7) Grosso M., Motta A., Rigamonti L., *Waste Manag.*, **30**, 1238–1243 (2010).
8) Fu H., Matthews M. A., *J. Hazard. Mater.*, **67**, 197–213 (1999).
9) Løvik A. N., Hagelüken C., Wäger P., *Sustain. Mater. Technol.*, **15**, 9–18 (2018).

10) Hu X., Wang C., Lim M. K., Koh S. C. L., *J. Clean. Prod.*, **243**, 118576 (2020).
11) Nygaard A., *Circ. Econ. Sustain.*, **3**, 1099–1126 (2023).
12) Nuss P., Harper E. M., Nassar N. T., Reck B. K., Graedel T. E., *Environ. Sci. Technol.*, **48**, 4171–4177 (2014).
13) Singh K., Khatirkar R. K., Sapate S. G., *Wear*, **328–329**, 206–216 (2015).
14) Hagedorn W., Jäger S., Wieczorek L., Kronenberg P., Greiff K., Weber S., Roettger A., *J. Clean. Prod.*, **377**, 134439 (2022).
15) Bocchini G. F., *Powder Metall.*, **26**, 101–113 (1983).
16) Yang Y. F., Qian M., "Titanium Powder Metallurgy," Elsevier, 2015, pp.219–235.
17) Mamedov V., *Powder Metall.*, **45**, 322–328 (2002).
18) Munir Z. A., Anselmi-Tamburini U., Ohyanagi M., *J. Mater. Sci.*, **41**, 763–777 (2006).
19) Tomohiro Y., Threrujirapapong T., Hisashi I., Katsuyoshi K., *Trans. JWRI*, **38**, 37–41 (2009).
20) Kim D. K., Pak H.-R., Okazaki K., *Mater. Sci. Eng. A*, **104**, 191–200 (1988).
21) Musa C., Licheri R., Locci A. M., Orrù R., Cao G., Rodriguez M. A., Jaworska L., *J. Clean. Prod.*, **17**, 877–882 (2009).
22) Maccari F., Mishra T. P., Keszler M., Braun T., Adabifiroozjaei E., Radulov I., Jiang T., Bruder E., Guillon O., Molina-Luna L., Bram M., Gutfleisch O., *Adv. Eng. Mater.*, (2023).
23) Bram M., Jäger S., Mishra T. P., Röttger A., Weber S., Field Assisted Sintering Technique/Spark Plasma Sintering (FAST/SPS) as promising method for upcycling of waste materials, 2021.
24) Salunkhe S., Fabijanic D., Nayak J., Hodgson P., *Mater. Today Proc.*, **2**, 1901–1906 (2015).
25) Chawake N., Pinto L. D., Srivastav A. K., Akkiraju K., Murty B. S., Kottada R. S., *Scr. Mater.*, **93**, 52–55 (2014).
26) Großwendt F., Bürk V., Kopanka B., Jäger S., Pollak S., Leich L., Röttger A., Petermann M., Weber S., *J. Clean. Prod.*, **392**, 136329 (2023).

Received June 26, 2024; Revised August 26, 2024; Accepted September 9, 2024